Low-Lying Neutron Intruder State in ^{13}B and the Fading of the $N = 8$ Shell Closure

H. Iwasaki,[1] A. Dewald,[1] C. Fransen,[1] A. Gelberg,[1] M. Hackstein,[1] J. Jolie,[1] P. Petkov,[1,2] T. Pissulla,[1] W. Rother,[1] and K. O. Zell[1]

[1]*Institut für Kernphysik, Universität zu Köln, D-50937 Köln, Germany*

[2]*Institute for Nuclear Research and Nuclear Energy, Bulgarian Academy of Sciences, 1784 Sofia, Bulgaria*

(Received 19 January 2009; revised manuscript received 28 April 2009; published 22 May 2009; publisher error corrected 5 June 2009)

A lifetime measurement of the excited states in the neutron-rich isotope ^{13}B has been performed using the ^{7}Li(^{7}Li, p)^{13}B reaction. An anomalously long mean lifetime of 1.3(3) ps was found for the excited state at 3.53 MeV, giving the upper limits of the transition strengths to the ground state: $B(M1) = 7.2 \times 10^{-4}$ Weisskopf unit (W.u.) and $B(E2) = 0.81$ W.u.. The hindered transition strengths indicate significant intruder configurations for the excited state, coexisting with the normal ground state. The data are well explained by recent shell-model calculations, which suggest $J^{\pi} = 3/2^{-}$ for the 3.53-MeV state with the dominant intruder ($\nu 2p2h$) configuration.

DOI: 10.1103/PhysRevLett.102.202502 PACS numbers: 21.10.Tg, 23.20.Js, 25.70.Hi, 27.20.+n

The isospin dependence of the nuclear shell structure represents a unique and intriguing feature of atomic nuclei as a finite fermion system composed of protons and neutrons. In this respect, the drastic evolution of the shell structure observed among neutron-rich nuclei with the neutron number $N = 8$ is of considerable interest [1–7]. The closed p-shell structure is pronounced in the doubly magic $N = Z$ ^{16}O and the semimagic ^{14}C, while, in the neighboring neutron-rich even-even nucleus ^{12}Be, the intruder sd-shell configurations start to dominate the ground state [1,2] and the low-lying excited states [3,4]. The observed trend of the shell evolution thus provides an important benchmark for present nuclear structure theory, which involves the effects of the proton-neutron interactions, in particular, the proton-neutron monopole interaction [5,6]. The question that still remains open is to what extent universality of the shell evolution holds in this neutron-rich region around $N = 8$.

If one looks at the $N = 8$ line, the ^{13}B isotope attracts a lot of attention because of its unique location between ^{14}C and ^{12}Be, where a global trend of the rapid shell evolution is anticipated to manifest itself. The ground state has the spin and parity (J^{π}) of $3/2^{-}$ [8]. Its magnetic dipole moment is close to the Schmidt limit, suggesting the dominant $(\pi 1p_{3/2})^{-1}$ configuration [8]. A small admixture of the sd-shell configuration in the ground state was suggested in Ref. [9]. However, the excited states are not well known experimentally. Below the neutron separation energy of 4.87 MeV, six excited states were observed at around 4 MeV, and partial information on spin and parity was obtained from the transferred angular momenta (ΔL) in the ^{11}B(t, p)^{13}B reaction [10]. Only recently, J^{π} of the 4.83-MeV state was determined to be $1/2^{+}$ in the ^{4}He(^{12}Be, ^{13}Bγ) study [11]. The $1/2^{+}$ state, interpreted as a proton intruder state [11], indicates a presence of the ($\pi 1p1h$) and ($\nu 2p2h$) configurations, pointing to the complex structure of ^{13}B. Among the cross-shell excitations predicted by the shell model [6,12,13], the $3/2^{-}$ excited state involving the coupling of $(\pi 1p_{3/2})^{-1}$ to the intruder ($\nu 2p2h$) configuration is of special interest, because the occurrence of the state at low excitation energy indicates a reduced $N = 8$ shell gap between the p and sd shells.

In this Letter, we report on a lifetime measurement of the excited states in ^{13}B by the Doppler-shift attenuation method (DSAM). In the previous DSAM work on ^{13}B [14], the γ-ray spectrum suffered from high background, limiting the accuracy of the lifetime measurement. The present work employs the particle-γ coincidence to select the reaction channel unambiguously and hence to reduce considerably the background. We use a hindrance of electromagnetic transitions, in comparison with empirical strengths and shell-model calculations, in order to identify intruder states.

The experiment was performed at the FN Tandem facility of the University of Cologne. Excited states in ^{13}B were populated using the ^{7}Li(^{7}Li, p)^{13}B reaction at a beam energy of 5.4 MeV. The target consisted of a 0.14 mg/cm^2-thick ^{7}LiF layer deposited onto a 2.1 mg/cm^2-thick Au foil. As shown in Fig. 1, the setup consisted of one EUROBALL cluster Ge detector [15] at 0° with respect to the beam axis and five large volume coaxial Ge detectors at an angle of 140°, each having an efficiency of about 60%. The target-detector distance was

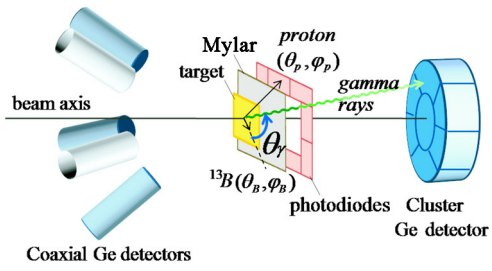

FIG. 1 (color online). A schematic drawing of the setup.

 © 2009 The American Physical Society

about 20 cm. In order to enable particle-γ coincidences, eight Si photodiodes, with the size of 5 mm $\times$ 10 mm, were positioned downstream of the target. For simplicity, each pair of them was electronically connected and used as a single detector. The particle detector covered the laboratory scattering angles from 62° to 81°. A thin Mylar foil with the thickness of 1.3 mg/cm^2 was introduced between the target and the particle detectors to prevent the scattered beam from hitting the detectors.

In order to apply the DSAM, the γ-ray emission angle θ_γ was obtained from the angle between the direction of the reaction product (^{13}B) and the axis from the target to the γ-ray detector. The hit pattern of the particle detectors was used to deduce the emission angle (θ_p, ϕ_p) of the ejected proton (Fig. 1), where θ_p and ϕ_p denote the polar and azimuthal angles, respectively. The emission angle (θ_B, ϕ_B) of ^{13}B was obtained from (θ_p, ϕ_p) using kinematics. θ_γ was thus determined for each combination of the 12 γ-ray detectors and the four particle signals. The symmetry of the setup allowed one to group the data into the four sets labeled as A, B, C, and D. θ_γ (and its rms) in the ^{7}Li(^{7}Li, p)^{13}B reaction was obtained as 17°(8°) for A, 34°(5°) for B, 134°(8°) for C, and 160°(8°) for D, by a Monte Carlo simulation incorporating the geometry of the setup and the reaction kinematics.

In the present study, the reaction channels were identified by using a correlation between the measured energies for the light particles and γ rays. This is demonstrated in Fig. 2(a), where the correlation in group A is compared to the kinematics conditions for the two-body reactions: ^{7}Li(^{7}Li, p)^{13}B (the light shaded area) and ^{7}Li(^{7}Li, d)^{12}B (the dark shaded area). The calculations assume that the reaction populates the observed states directly, and take into account the angular acceptance of the particle detectors, the energy loss of the light particles in the target, and the Mylar foil, as well as possible Doppler shifts in the γ-ray energies. In Fig. 2(a), five loci, corresponding to the known excited states in ^{13}B at 3.53, 3.68, 3.71, 4.13, and 4.83 MeV [10], are evident and clearly separated from background contributions in the low energy region. The correlation for the two states in ^{12}B at 0.95 and 1.67 MeV is also consistent with the calculation, while the separation is less clear. The three loci with the γ-ray energies of around 2.17, 4.54, and 5.12 MeV are attributed to the three lowest excited states in ^{11}B populated by the ^{7}Li(^{7}Li, t)^{11}B reaction. The double-escape peak of the 4.54-MeV γ rays appears at 3.52 MeV, overlapping with the 3.53-MeV locus for ^{13}B on the plot of Fig. 2(a), while the 3.52-MeV contaminant in the shaded area was clearly separated and found to be less than 10% of the 3.53-MeV component.

The γ-ray spectrum gated with the kinematics condition for ^{13}B is shown in Fig. 2(b). For comparison, we plot, in Fig. 2(c), the spectrum obtained by setting a gate close to the ^{13}B area. The five transitions in ^{13}B are evident only in Fig. 2(b), while the background peaks are visible in both Figs. 2(b) and 2(c). Based on the cross sections predicted

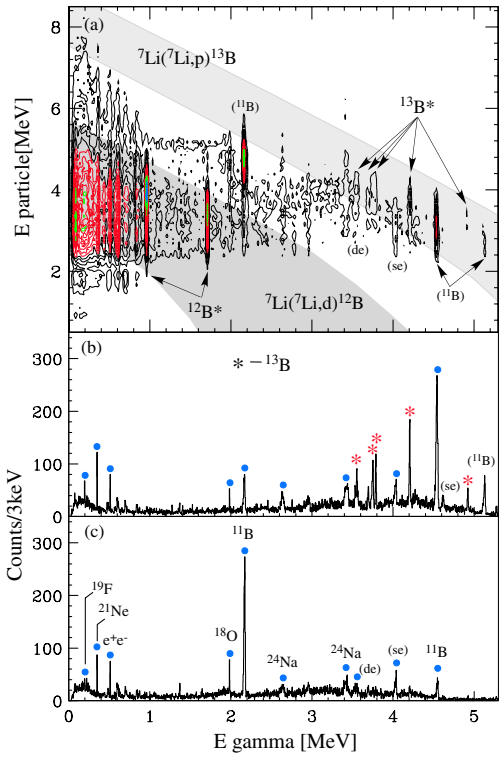

FIG. 2 (color online). (a) The correlation between the measured light-particle and γ-ray energies. (b) The γ-ray spectrum for ^{13}B. (c) The representative background spectrum (see text). In (b) and (c), the γ transitions for ^{13}B and other nuclei are indicated by the stars and circles, respectively. The labels (se) and (de) mean the single-escape and double-escape peaks, respectively.

by the CASCADE code [16], the background γ rays are mainly associated with the products of the ^{7}Li + F reaction as indicated in Fig. 2(c).

In order to obtain the mean lifetime (τ) of the observed states, we first compare, in Fig. 3(a), the measured and simulated γ-ray energies. The background was subtracted using the data shown in Fig. 2(c). As indicated by the level scheme for ^{13}B, we observed the ground-state transitions from the five excited states at around 4 MeV except for the first excited state at 3.48 MeV. The measured γ-ray energy E_γ can be written as $E_\gamma = E_\gamma^0[1 + \beta_i F(\tau)\cos\theta_\gamma]$, with E_γ^0 being the unshifted γ-ray energy, β_i the initial velocity with respect to the light velocity, θ_γ the γ-ray emission angle, and $F(\tau)$ the attenuation factor. The γ-ray peak of the 3.53-MeV transition is close to the unshifted energy with $F(\tau) = 0$, while the other four peaks appear at around the full-Doppler-shifted energies with $F(\tau) = 1$, indicating remarkable differences among the lifetimes of the states.

The lifetime of the 3.53-MeV state was obtained by analyzing the γ-ray line shape as shown in Fig. 3(b). We performed the Monte Carlo simulation [17–19], which incorporates the electronic and nuclear stopping processes, the reaction kinematics, as well as the geometry of the setup. The electronic stopping power was obtained by the

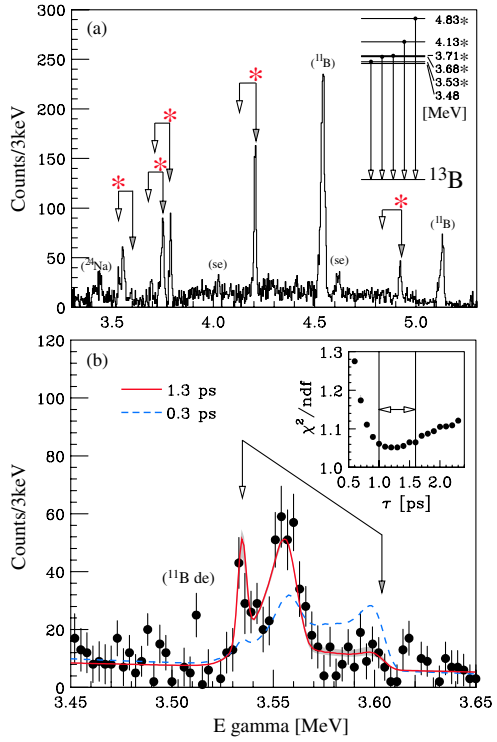

FIG. 3 (color online). (a) Background subtracted γ-ray spectrum for ^{13}B measured in group A. The open arrows and closed arrows denote the unshifted and full-Doppler-shifted γ-ray energies, respectively. (b) The fits to the data of the 3.53-MeV transition. The solid curve and the dashed curve show the results with $\tau = 1.3$ ps and 0.3 ps, respectively. The inset shows the reduced χ^2 distribution as a function of τ. The shaded area in the spectrum and the arrows in the inset represent the error.

SRIM code [20]. The nuclear stopping and scattering were derived from an approximation to the universal scattering function [17]. We took the normalization factors $f_e = 1.1$ and $f_n = 1.0$ [21] for the electronic and nuclear stopping powers, respectively, where the former was obtained by comparing the SRIM tables with the data for the B ions [14]. We used the data from group A, which has the highest sensitivity and is free from any escape peak of the neighboring transitions. The solid curve in Fig. 3(b) shows the best-fit result with $\tau = 1.3$ ps. Because of the long lifetime, parts of the excited ^{13}B nuclei can pass through the Au foil, producing a broad shifted peak at around 3.56 MeV in addition to the unshifted peak at 3.53 MeV and the fast-moving component starting from 3.60 MeV. In the inset of Fig. 3(b), the reduced χ^2 distribution of the fit is shown from 0.6 to 2.3 ps in 0.1 ps steps. The lifetime of the 3.53-MeV state is thus determined to be $\tau = 1.3(3)$ ps, which is about 4 times longer than the previous lower limit of $\tau = 0.3$ ps [14].

The other lifetimes were studied by analyzing the centroid shifts of the observed γ-ray peaks. The data from all the groups (A–D) were used. $F(\tau) = 0.93(1)$ was obtained for the 3.68-MeV state in ^{13}B giving $\tau = 55(20)$ fs. No substantial attenuation smaller than 0.96 was found for the other three transitions in ^{13}B, which places the upper limits at $\tau < 30$ fs. In deducing the lifetime of the 3.53-MeV state, we neglected effects due to possible cascade transitions, which were not evident in the present work. However, the short lifetimes obtained for the states above 3.53 MeV hardly affect the result of the 3.53-MeV state. The validity of the present work was tested by analyzing the known lifetime of the 0.95-MeV state in ^{12}B. The $F(\tau)$ value was obtained to be 0.54(2), giving $\tau = 285(20)$ fs, which is in good agreement with the former result of 295(37) fs [14].

The electromagnetic transition strengths were deduced from the lifetimes of the 3.53- and 3.68-MeV states in ^{13}B. In the ^{11}B$(t, p)^{13}$B reaction [10], the 3.53- and 3.68-MeV states were populated with the transferred angular momenta $\Delta L = 2$ and $\Delta L = 1$ from the ground state of ^{11}B with $J^\pi = 3/2^-$, respectively. Both $M1$ and $E2$ transitions are possible for the 3.53-MeV transition to the ground state of ^{13}B with $J^\pi = 3/2^-$. The upper limits of the strengths are thus determined from τ of 1.3(3) ps to be $B(M1) = 1.3 \times 10^{-3} \mu_N^2$ or 7.2×10^{-4} Weisskopf unit (W.u.), and $B(E2) = 1.5\ e^2\,\mathrm{fm}^4$ or 0.81 W.u., independently of the mixing ratio δ. For the 3.68-MeV transition, $\tau = 55(20)$ fs gives $B(E1) = 2.3(8) \times 10^{-4}\ e^2\,\mathrm{fm}^2$ or $6.4(23) \times 10^{-4}$ W.u.. Typical transition strengths in the mass region of $A = 6$–20 are 10^{-4}–10^{-1} W.u. ($E1$), 10^{-2}–10^{1} W.u. ($M1$), and 10^{-1}–10^{2} W.u. ($E2$) [22]. The present upper limit of $B(M1)$ of 7.2×10^{-4} W.u. for the 3.53-MeV state highlights an anomalously hindered strength, suggesting substantial intruder configurations regardless of the spin and parity of the state.

In order to better understand the underlying structure, we carried out shell-model calculations using the OXBASH code [23]. We used an advanced Hamiltonian (called *present'* in Ref. [6]), which included an improved proton-neutron monopole interaction. The configuration space is taken up to $4\hbar\omega$ so as to reproduce well the location of the intruder states in ^{11,12}Be [6]. The bare g factors and the effective charges of $e_p = 1.5$ and $e_n = 0.5$ were used. In Fig. 4(a), our results on $B(M1)$ and $B(E2)$ for the 3.53-MeV transition are compared with the theoretical values. The four lowest negative-parity states below 6.5 MeV, which have $J^\pi = (1/2^-, 3/2^-, 5/2^-, 7/2^-)$, are chosen from the shell-model calculations as candidates for the 3.53-MeV state [10]. The hindered strengths for the 3.53-MeV transition are only consistent with $J^\pi = (3/2^-, 7/2^-)$. The dominant $(\nu 2p2h)$ configuration in the $3/2^-$ excited state causes the hindrance of the transition strengths to the ground state with the dominant $(\nu 0p0h)$ character. In the case of $J^\pi = (1/2^-, 5/2^-)$, the transition involves substantial spin-flip excitations between the $1p_{3/2}$ and $1p_{1/2}$ states, resulting in large $B(M1)$ strengths.

The excitation energy is compared with the shell-model calculations in Fig. 4(b). The calculated $3/2^-$ excited state in ^{13}B is very close to the 3.53-MeV state, while the $7/2^-$

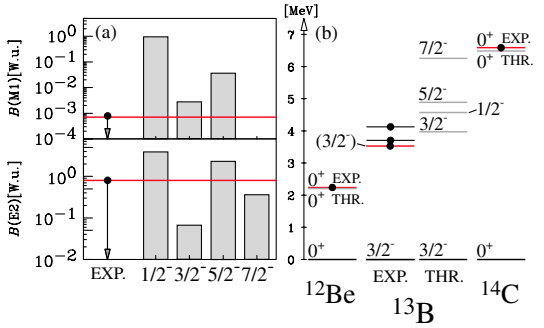

FIG. 4 (color online). (a) The upper limits of $B(M1)$ and $B(E2)$ for the 3.53-MeV transition are shown by the lines with the arrows and compared with the calculated strengths between the lowest $(1/2^-, 3/2^-, 5/2^-, 7/2^-)$ excited states and the $3/2^-$ ground state. (b) Partial level schemes in $N = 8$ isotones. The lines with the dots and the thin lines represent the experimental and theoretical levels, respectively. Only negative-parity bound states at 3.53, 3.71, and 4.13 MeV [10] are shown for the experimental levels of ^{13}B.

state in the shell model is located at a very high energy as is the case in other theoretical works [7,12,13]. Thus, J^π of the 3.53-MeV state is most likely $3/2^-$. The present calculations also reproduce well the location of the 0_2^+ states in ^{12}Be [6], and ^{14}C in this work.

Following Refs. [4,24,25], the configurations of the last two neutrons in the two $3/2^-$ (0^+) states of ^{13}B (^{12}Be, ^{14}C) can be written as $|\nu_1\rangle \simeq \alpha|(p)^2_{J=0}\rangle + \beta|(sd)^2_{J=0}\rangle$ (the ground state) and $|\nu_2\rangle \simeq -\beta|(p)^2_{J=0}\rangle + \alpha|(sd)^2_{J=0}\rangle$ (the excited state) with $\alpha^2 + \beta^2 = 1$, both of which are coupled to the $1p_{3/2}$ protons. We note that, in the present shell-model calculations, the presence of other configurations such as $|(sd)^2_{J=2}\rangle$ in the excited state is important for explaining the hindered, but nonzero $M1$ and $E2$ transition strengths in ^{13}B. The shell-model results agree with the ground-state properties of ^{13}B (^{14}C) with $\alpha^2 = 0.7$–0.8 [9,24] ($\alpha^2 \sim 0.9$ [25]), and of ^{12}Be with $\alpha^2 \sim 0.3$ [1,2]. It is striking that the excitation energies and the amplitudes of the neutron intruder states change drastically from ^{14}C via ^{13}B to ^{12}Be by just removing one proton from the $1p_{3/2}$ orbit. The rapid shell quenching confirmed in the $N = 8$ isotones, as well as similar trends observed in the $N = 7$ [26] and $N = 9$ [9] isotones, upholds the universality of the shell evolution in the neutron-rich nuclei around $N = 8$. This supports the important role of the proton-neutron monopole interaction between the two orbits $\pi 1p_{3/2}$ $(j_>)$ and $\nu 1p_{1/2}$ $(j_<)$ [5,6].

In the study of the ^{11}B$(t, p)^{13}$B reaction [10], the J^π assignment of $3/2^-$ was considered to be unlikely for the 3.53-MeV state among possible candidates of $J^\pi = (1/2^-, 3/2^-, 5/2^-, 7/2^-)$, because the population mainly occurred via the $\Delta L = 2$ transition. However, there is no contradiction with the present discussion, because the shell-model wave function includes the $\nu|(sd)^2_{J=2}\rangle$ configuration to be populated by $\Delta L = 2$.

The neutron intruder $3/2^-$ state as suggested for the 3.53-MeV state, together with the proton intruder $1/2^+$ state at 4.83 MeV [11], represents an intriguing example of coexisting proton and neutron intruder configurations as well as the normal configuration in the ground state. Further experimental and theoretical efforts would be of interest to understand a possible shape coexistence of this nucleus, which has recently been proposed by the antisymmetrized molecular dynamics calculations [7].

In summary, we have indicated the first evidence for the intruder $3/2^-$ state in ^{13}B at 3.53 MeV which involves the dominant $(\nu 2p2h)$ configuration. The hindered transition strengths between this excited state and the $3/2^-$ ground state highlight the coexisting normal and intruder configurations, depicting a clear illustration of the fading of the $N = 8$ shell closure in the neutron-rich isotope ^{13}B.

The authors would like to thank Professor Toshio Suzuki for permission to use the shell-model interaction. One of the authors (H. I.) would like to acknowledge the support from the Alexander von Humboldt foundation.

[1] A. Navin *et al.*, Phys. Rev. Lett. **85**, 266 (2000).
[2] S. D. Pain *et al.*, Phys. Rev. Lett. **96**, 032502 (2006).
[3] H. Iwasaki *et al.*, Phys. Lett. B **481**, 7 (2000); H. Iwasaki *et al.*, Phys. Lett. B **491**, 8 (2000).
[4] S. Shimoura *et al.*, Phys. Lett. B **560**, 31 (2003); S. Shimoura *et al.*, Phys. Lett. B **654**, 87 (2007).
[5] T. Otsuka *et al.*, Phys. Rev. Lett. **87**, 082502 (2001).
[6] T. Suzuki, R. Fujimoto, and T. Otsuka, Phys. Rev. C **67**, 044302 (2003).
[7] Y. Kanada-Enyo *et al.*, Prog. Theor. Phys. **120**, 917 (2008).
[8] R. L. Williams, Jr. and L. Madansky, Phys. Rev. C **3**, 2149 (1971).
[9] N. Aoi *et al.*, Phys. Rev. C **66**, 014301 (2002).
[10] R. Middleton and D. J. Pullen, Nucl. Phys. **51**, 50 (1964).
[11] S. Ota *et al.*, Phys. Lett. B **666**, 311 (2008).
[12] A. A. Wolters *et al.*, Phys. Rev. C **42**, 2062 (1990).
[13] V. Guimarães *et al.*, Phys. Rev. C **61**, 064609 (2000).
[14] M. J. Throop, Phys. Rev. **179**, 1011 (1969).
[15] J. Eberth *et al.*, Prog. Part. Nucl. Phys. **38**, 29 (1997).
[16] F. Pühlhofer, Nucl. Phys. **A280**, 267 (1977).
[17] W. M. Currie, Nucl. Instrum. Methods **73**, 173 (1969).
[18] G. Winter, Nucl. Instrum. Methods **214**, 537 (1983).
[19] P. Petkov *et al.*, Nucl. Instrum. Methods Phys. Res., Sect. A **431**, 208 (1999).
[20] J. F. Ziegler *et al.*, http://www.srim.org.
[21] T. R. Fisher *et al.*, Phys. Rev. **176**, 1130 (1968).
[22] P. M. Endt, At. Data Nucl. Data Tables **23**, 3 (1979).
[23] Computer code OXBASH, in B. A. Brown, A. Etchegoyen, and W. D. M. Rae, MSU-NSCL Report No. 524, 1986.
[24] H. T. Fortune and R. Sherr, Phys. Rev. C **68**, 024301 (2003).
[25] H. T. Fortune and G. S. Stephans, Phys. Rev. C **25**, 1 (1982).
[26] I. Talmi and I. Unna, Phys. Rev. Lett. **4**, 469 (1960).